Civil Engineering and Architecture 1(1): 20-32, 2013 http://www.hrpub.org
DOI: 10.13189/cea.2013.010103

Towards Improved Engineering Model for Sediment Transport Prediction Under Combined Wave-Current Sheet Flows

Ming Li

Centre for Engineering Sustainability, School of Engineering, the University of Liverpool,
Brownlow Street, Liverpool, L69 3GQ, United Kingdom
*Corresponding Author: mingli@liv.ac.uk

Abstract Sediment transport under combined wave-current sheet flow condition is predicted by a wave-period-averaged (WPA) profile model based on a diffusion concept. The total transport rate is split into current induced and wave induced components with associated model parameters. The current induced transport rate is evaluated through vertical profiles of wave-period-averaged flow velocity and sediment concentration. A new wave-induced transport profile is also proposed utilising the wave-induced current residual velocity and period-averaged sediment concentrations. Important sheet flow processes, including turbulence dumpling in the suspension layer, sediment particle's hindered settling and phase-lag effects are taken into account through a number of model parameters that have been validated by available laboratory measurements. Sediment size gradient is also considered by a conventional multi-fraction approach with special treatment for the sediment mixing parameters for fine and coarse sediment fractions. Model results for both laboratory and field measurements show its encouraging accuracy for the sediment transport prediction under sheet flow condition.

Keywords Sediment transport, Oscillatory sheet flow, Graded sediment, Numerical model, Sediment transport rate, Phase lag

1. Introduction

As the offshore wave propagates to the coasts, wave height and steepness will increase till wave breaking takes place. The near bed orbital velocity will also increase as the surface wave becomes increasingly non-linear. When the velocity become so large that the shear parameter is larger than 1.0, all seabed features, such as ripples will be washed out and sand is transported close to the plane bed surface in a thin sheet with thickness of few mm to cm, i.e. the so called sheet flow regime. In this case the near bed velocity and sediment concentration are very high, the total transport rate is therefore significant comparing with other conditions which often plays an important role in determine the local beach profile configuration.

However, to predict sediment transport in combined wave-current oscillatory sheet-flows is still a challenging research subject for coastal engineers, especially for situations involving fine and graded sediment materials. Numerous laboratory and theoretical studies have been carried out in recent years in order to improve the existing prediction method, for example the series experiments conducted in the oscillatory tunnel at LOWT, Delft Hydraulics since 1990s (Katopodi et al [14], Ribberink and Al-Salem [21], Janssen et al [12], Hamm et al [10], Dohmen-Janssen [5] and Trouw et al [27]) and more recently at AOFT, the University of Aberdeen (O'Donoghue and Wright [20], van et al A [28], van der A et al [29]), as well as the numerical model developments by Dibajnia and Watanabe [4], Li and Davies [17], Savioli and Justesen [24], Malarkey et al. [18] and Ruessink et al [23]. These activities indicate the need to incorporate sheet flow layer processes into the numerical model framework so that the transport rate can be predicted with reasonable accuracy. However, the lack of detailed knowledge of sediment transport mechanisms in combined flows prevents significant progress towards improved engineering models (van Rijn et al. [35]). In contrast, the complex nature of sheet flow tends to require the use of very sophisticated numerical approaches, for example the multi-phase model of Li and Sawamoto [15], Dong and Zhang [7], Hsu et al [11], Li et al [16] and more recent Yu et al [38]. Such complicated models are likely to be time consuming and less attractive from the practical application point of view. More recent development in study of sheet flows under skewed waves within the SANTOSS project (van der A et al [30]) provides promising approach in which prediction method is developed based on semi-empirical formulation of intra-wave process, including effects from wave asymmetry, phase lag and surface

oscillation. Test of the model by van der Werf [31] has shown its potential in prediction of wave induced beach profile changes. However, the SANTOSS model is largely designed for wave induced sheet flows, concentrating on the bed load region. Details of the suspended load at the level higher up in the water column are not given explicitly by the model, which often is critical for situation that suspended transport is dominant.

The present study, therefore, aims to develop a model for the prediction of transport rates in combined wave and current induced sheet flows based on wave-period-averaged (WPA) velocity and concentration profiles from the initial still bed level up to the free surface and no distinguish is made between bed load and suspended load. The total transport rate is split into current induced and wave induced components. The current induced transport is computed using the wave-period-averaged characteristics and the wave induced transport is evaluated based on a WPA transport flux profile. The sum of these two transport fractions provides a total transport rate. By using WPA values, the present method does not need to evaluate the intra-wave information, which is different from the SANTOSS model and much simplified the procedure. The results clearly demonstrate the importance of intra-wave processes to the overall net sediment transport rate, such as shear flow processes, wave asymmetry and sediment size grading. However, different from many existing works, the present study includes these complex physics in the simple 1D model based on WPA approach through several parameters, which clearly is beneficial for engineering applications, particularly from the long term morphological modeling point view. After calibration, model tests for both laboratory and field conditions also demonstrate its capability in practical applications. The paper is organised as follows: in Section 2 a brief description of oscillatory sheet flow processes is presented, Section 3 discusses theoretical background of the present model, following with model parameterisations and calibration in Section 4. Model results are then compared with measurements in Section 5 and finally some conclusions are given at Section 6.

2. Oscillatory Sheet Flow Processes

In the oscillatory sheet flows, sediment suspension occurs in distinct layers, i.e. a pick-up layer, an upper sheet flow layer and a suspension layer (Dohmen-Janssen [5]). In each layer, the sediment particles exhibit very different behavior, which significantly complicates the prediction method.

Immediately above the stationary bed is the pick-up layer. Within this layer, sediments are subject to intensive inter-particle collisions due to the high concentration. The instantaneous stationary bed position also varies along with the oscillatory flow forces. The resulted time history of sediment concentration is more or less in-phase with the oscillatory orbital motion.

As sediment particles being lifted up from the pick-up layer into the upper sheet flow layer, fluid-particle interaction becomes important for these materials to remain in suspension. A strong anti-phase tendency is found in the concentration time series comparing with the free orbital motion. An interesting common feature observed in existing laboratory data is that the sediment concentration at the undisturbed bed level tends to remain constant throughout the wave cycle, which indicates the influences from fluid shear forces are less obvious at this level, in contrast to the theory for the existing numerical sediment transport models (Dohmen-Janssen [5], O'Donoghue and Wright [20], van der A et al [28]). As far as the fluid flow is concerned, the high sediment concentration certainly reduces the turbulence level and hence leads to low mixing characteristics compared with that in a pure fluid flow.

Higher above the sheet flow layer is the suspension layer in which diffusion due to fluid turbulence dominant the sediment transport. Meanwhile, many research studies have recognized that flow stratification, damping of turbulence and hindered settling in the suspension layer play a vital role in the concentration distribution, see Li and Davies [17].

3. Numerical Model

Following many existing models, the mechanism for sediment transport under combined waves and current is simplified as the waves stir up sediment into suspension and the current transport sediment particles within the water column. Therefore, the net transport can be split into a current-related and a wave-related component:

$$q_s = q_c + q_w = \int_0^h \overline{u}_c \overline{C} dz + \int_0^h \overline{u}_w \overline{C} dz \qquad (1)$$

where q_s is total transport rate, q_c and q_w are current-related and wave-related transport rate respectively, h is water depth, $\overline{u}_c$ and $\overline{u}_w$ denote current- and wave-induced wave-period-averaged net drift flow velocity respectively and $\overline{C}$ is the wave-period-averaged sediment concentration. Details of the current-induced and wave-induced WPA velocity profiles and sediment concentration distribution are given in the following sections.

3.1. Eddy Viscosity and Current-Induced WPA Velocity Profile

Many models are available in the literature for calculation of the WPA velocity profile in combined wave-current flows, for example Fredsøe [8], O'Connor and Yoo [19], van Rijn [33], Sleath [25] and Soulsby [26]. In the present study, the You et al. [37] and You [36] approach is adopted after comparison with a number of measurements. In this method, two logarithmic profiles are described according to the given wave-current characteristics and a measured or known velocity value at a particular point

outside the wave boundary layer. This method is relatively straightforward to use since no iteration is required.

Based on available laboratory measurements, however, it is also found necessary to introduce some modifications into the velocity profile description of You [36] in sheet flow condition. First of all, for the wave induced oscillatory boundary layer, the thickness of the layer needs to be determined as $\delta_w = 0.0465A(k_s / A)^{0.172}$, where A is the wave-induced orbital excursion diameter and ks is the bed roughness height (Fig 1a). Based on many existing measurements, the eddy viscosity is then proposed as follows:

$$\varepsilon_f = \begin{cases} \kappa\beta_c u_{sw} z & \text{for } z_0 \le z \le 0.5\delta_w \\ 0.5\kappa\beta_c u_{sw}\delta_w & \text{for } 0.5\delta_w \le 2\delta_w \\ \kappa\beta_c u_{fc} z\left(1-\dfrac{z}{h}\right) & \text{for } 2\delta_w \le z \le h \end{cases} \quad (2)$$

where ε_f is fluid eddy viscosity, z is the vertical coordinate starting from the initial bed level upwards towards the water surface, $u_{sw} = \sqrt{0.5 f_w}\, A\omega$ is wave-induced shear velocity inside boundary layer, ω is angular frequency of the wave, $f_w = 0.108(A/k_s)^{-0.343}$ is wave friction factor, $z_0 = k_s/30$ is the level of velocity equal to zero, β_c is the eddy viscosity reduction parameter, $\kappa = 0.4$ is the von Karman constant and u_{fc} is the apparent shear velocity outside the boundary layer due to wave-current interaction, which is computed as

$$u_{fc} = \frac{-B_1 + \sqrt{B_1^2 - 4A_1C_1}}{2A_1} \quad \text{and} \quad A_1 = \frac{\ln(e\delta_w / z_0)}{u_{sw}},$$

$B_1 = \ln\left(\dfrac{z_r}{2\delta_w}\right)$ and $C_1 = -kU_r$, where U_r is a known flow velocity at a given level z_r.

Assume a linear distribution of the shear stress across water column, the wave-period-averaged flow velocity due to current can then be decided as in Fig 1(c): below a level of half of the boundary layer thickness, the current velocity is computed using a logarithmic function taking wave-current interaction into account. Above twice of the boundary layer thickness, the flow velocity is described by another logarithmic profile with enhanced roughness (30z1) due to the presence of waves. The velocity profile between half to twice the boundary layer thickness is assumed to be a simple linear distribution, similar to the approach of Kaczmarek [13]. The difference between the above distribution and the scheme of You [36] lies in the fact that the thickness of the first layer in the original You [36]'s model is up to the whole wave boundary layer, rather than the half of it as in the present study. In addition, the present model also uses a linear profile to link the layer outside boundary layer and the lower layer within boundary layer. Above the $2\delta_w$ level, a parabolic type of eddy viscosity is used so that a linear shear stress distribution can be realised. In the You [36] paper, a simple linear eddy viscosity is employed which corresponds to a constant shear stress. These modifications are based on the existing measurements and also reflect the fact that the particle-fluid interaction becomes important in the upper sheet flow layer and suspension layer in comparison with the lower flow regime.

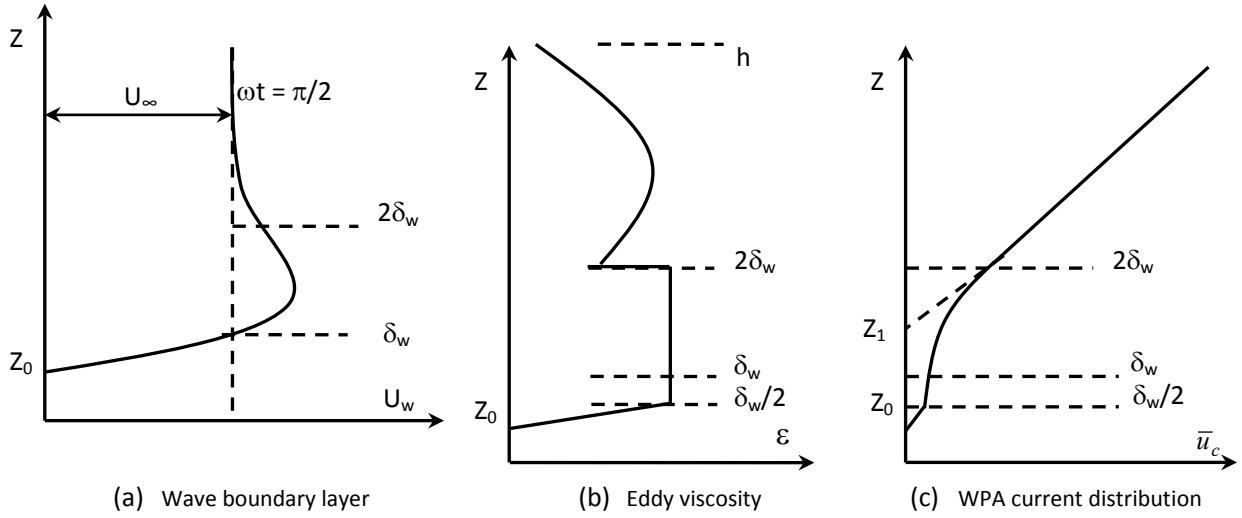

Figure 1. Definition of wave boundary layer, eddy viscosity and steady current distribution.

$$\overline{u}_c = \begin{cases} 0 & \text{for } z \le z_0 \\ \dfrac{u_{fc}}{\beta_c \kappa}\left(\dfrac{u_{fc}}{u_{sw}}\right)\ln\left[\dfrac{z}{z_0}\right] & \text{for } z_0 < z \le 0.5\delta_w \\ \dfrac{u_{fc}}{\beta_c \kappa}\left(\dfrac{u_{fc}}{u_{sw}}\right)\ln\left[\dfrac{0.5\delta_{sw}}{z_0}\right] + \dfrac{u_{fc}}{\beta_c \kappa}\left[\ln\left(\dfrac{2\delta_w}{z_1}\right) - \left(\dfrac{u_{fc}}{u_{sw}}\right)\ln\left[\dfrac{0.5\delta_w}{z_0}\right]\right]\dfrac{z-0.5\delta_w}{1.5\delta_w} & \text{for } 0.5\delta_w < z \le 2\delta_w \\ \dfrac{u_{fc}}{\beta_c \kappa}\ln\left(\dfrac{z}{z_1}\right) & \text{for } 2\delta_w < z \le h \end{cases} \tag{3}$$

where $z_1 = 2\delta_w\left(e\delta_w / z_0\right)^{-\lfloor u_{fc}/u_{sw}\rfloor}$ is the enhanced roughness parameter. It should be noted that the above profile is only applied down to the initial bed level (z=0). Laboratory evidence suggests the existence of erosion after one wave cycle and as a result the flow velocity is not zero below the initial bed level (O'Donoghue and Wright [20]). However, this process is not taken into account herein to avoid complex bed variation predictions as discussed in a later section.

In addition, previous studies of Li and Davies [17] and Dohmen-Jassen [5] have shown that the turbulence mixing is reduced as a result of the turbulence dumping due to the sediment stratification in sheet flows. To represent such effect properly, a reduction parameter β_c is specified in the eddy viscosity profile of You [36] across the water column, similar to the approach of Dohmen-Jassen [5].

Following Malarkey et al. [18], the bed roughness height k_s used in Eq.(1) for wave friction factor f_w and z_0 in sheet flows is specified according to the sand diameter and shear parameter θ as follows,

$$\frac{k_s}{d_{50}} = 2 + 3.2(\theta - 1) \quad \text{for } \theta > 1 \tag{4}$$

in which $\theta = u_{sw}^2 / [(s-1)gd_{50}]$ is the shear parameter, $s = \rho / \rho_s$ is the relative density of sediment, ρ is fluid density, ρ_s is density of sediment, d_{50} is median size of sediment, g is acceleration due to gravity. It is worth pointing out that the constant 3.7 in Malarkey et al. [18] is reduced to 3.2 after comparing with a number of measurements.

3.2 Wave-induced WPA velocity profile

Unlike the current-induced WPA velocity, it is difficult though to evaluate the wave-induced residual flow velocity. Based on examination of the available laboratory measurements, a profile of the wave residual velocity is proposed as shown in Fig 2, i.e. with an increase of the elevation from the bed, the velocity increases linearly from zero at the bed surface to its maximum at ¼δ_w in the onshore direction and then reversing back to the offshore direction reaching a peak at level of δ_w, followed by a constant value towards water surface:

$$\overline{u}_w = \begin{cases} 0 & \text{for } z \le 0 \\ \alpha U_{on}\dfrac{z}{\delta_w / 4} & \text{for } 0 < z \le 1/4\delta_w \\ \alpha U_{on} + \left[-\alpha U_{off} - \alpha U_{on}\right]\dfrac{z - 1/4\delta_w}{3/4\delta_w} & \text{for } 1/4\delta_w < z \le \delta_w \\ -\alpha U_{off} & \text{or } \delta_w < z \end{cases} \tag{5}$$

where U_{on} and U_{off} are the maximum onshore and offshore free stream velocity magnitude.

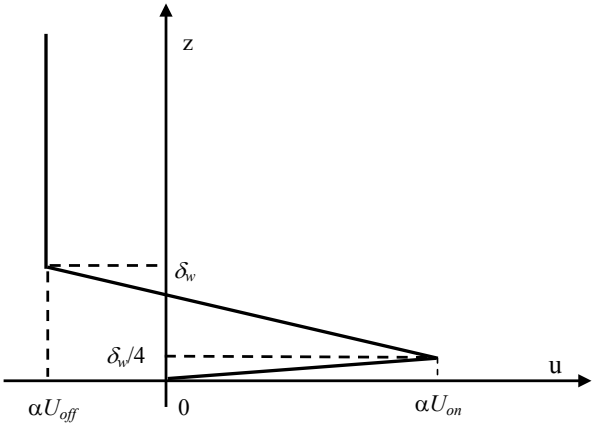

Figure 2. Scheme of residual wave velocity distribution.

The onshore residual flow at the lowest level is due to the Eulerian drift, i.e. wave-induced streaming under propagation waves over rough bed as shown in Davies and Villaret [2]. The offshore peak at a higher level is caused by the mass transport under surface wave propagation as demonstrated by many previous studies (Davies and Villaret [2]). In the present study, the magnitudes of these onshore and offshore velocity peaks are assumed to be proportional to the U_{on} and U_{off} via a parameter α, see Fig 2. After testing with different options, it was found that the α parameter can be related to a ratio between the thickness d_s for a layer close to the bed where concentration is linearly distributed (see later section 3.3 and Fig 3) and that for the wave boundary layer δ_w, i.e.

$$\alpha = \frac{1}{2}\frac{d_s}{\delta_w} \tag{6}$$

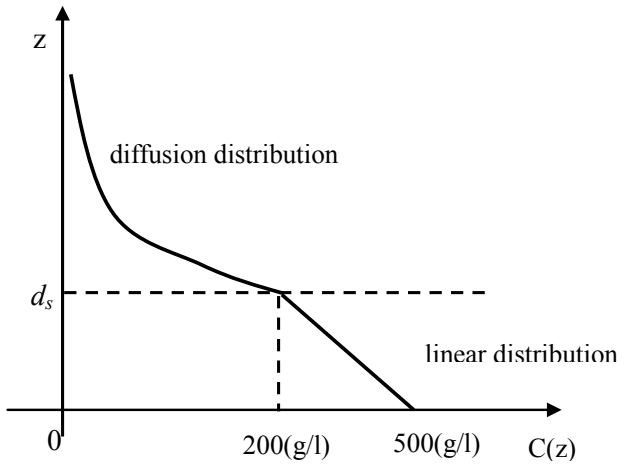

Figure 3. Scheme of wave-period-averaged sediment concentration distribution.

The above relationship also can be seen as an indication of the relative strength of wave oscillation to the total combined wave-current motion as thickness d_s for the first layer close to the bed, which is part of the sheet flow layer thickness, is proportional to the wave orbital strength. Grasmeijer *et al.* [9] suggested a wave-related transport rate formula based on wave asymmetry similar to Eq. (5). The assumption also has been made that the wave-related transport rate is proportional to the production of velocity due to wave asymmetry and WPA concentration. By comparison, the present approach is based on a description of a detailed wave-induced velocity profile across the water column. It is therefore possible to describe the physical processes with details at different levels above the bed.

3.3. WPA Concentration Profile

After the WPA flow velocity profile is established, the WPA sediment concentration profile can then be described based on the flow information. In the present study, a two-layer concentration distribution is used for the description of sediment suspension within the upper sheet flow layer and suspension layer (Fig 3). No consideration has been given to the pick-up layer. To this end, the assumption has been made that the majority of sediment transport takes place above the undisturbed bed level (z = 0). Although evidences from the existing laboratory measurements suggest that sediment particles remain mobile within the pickup layer under oscillatory sheet flows, especially for fine sediment materials, the large portion of the transport occurs higher in the upper sheet flow layer. Therefore, simplification is proposed in order to keep the present model focusing on overall sediment transport throughout the whole water column.

The sediment concentration shown in Fig 3 in the first layer above the bed is linearly distributed from 500g/l at z = 0 to 200g/l at a height (d_s). The reason for choosing 500g/l as reference concentration is based on data from the available laboratory measurements, commonly used in Dohmen-Janssen *et al* [6], O'Donoghue and Wright [20] and van der A [29]. The value of 200g/l concentration corresponds to the definition of the top of the sheet flow layer, which is 8% by volume (Dohmen-Janssen *et al* [6]). Due to the small variation range (200g/l – 500g/l) as well as the small value of d_s (order of a millimetre), the exact shape of the concentration within this layer may not be crucial, and the linear distribution therefore is simply chosen. The good agreement in model-data comparisons also to some extent verifies such an assumption as presented in a later section.

Above the first layer, the sediment concentration takes a diffusion distribution:

$$w_f \overline{C} + \varepsilon_s \frac{\partial \overline{C}}{\partial z} = 0 \tag{7}$$

in which $\overline{C}$ is the wave-period-averaged sediment concentration, w_f is a representative sediment fall velocity and β_s is the ratio between the sediment diffusivity and the standard fluid eddy viscosity. In general practice, the sediment diffusivity can be related to the eddy viscosity so that β_s is equal or proportional to the eddy viscosity parameter β_c in Eq. (2). However, unlike β_c which only accounts for the turbulence dumping, the β_s is also affected considerably by the hindered settling and sediment grain centrifugal effects. For a high concentration sediment–laden flow, the settling velocity has to be corrected to represent the inter-particles and particle-fluid interactions, as being indicated by many other studies (Li and Davies [17]). In addition, the sediment particles in the high concentration flows also are likely to be thrown outside the fluid turbulence eddy with increase of effective mixing, as suggested by van Rijn [34]. In the present study, these processes are also included into the β_s factor so that no further complications are involved. As a result, no similarity between β_s and β_c is drawn herein.

After inserting Eq. (8) into Eq. (7) and integrating over the water depth above the first layer, the following concentration distribution is obtained:

$$\overline{C} = c_b \left(\frac{z}{d_s} \right)^{-\left[\frac{w_f}{\beta_s \kappa u_{fc}} \right]} \qquad \text{for } z > d_s \tag{9}$$

where c_b is the near bed reference concentration (200g/l) as discussed above and d_s is the first layer thickness.

3.4. Total Transport Rate

It is also well known that for fine sand under wave induced sheet flows, a significant amount of sediment can be entrained from the bed by the strong onshore flow. But the time for these materials being diffused to a higher level is considerable in comparison with the wave period, and consequently a large proportion of these sands is transported in the subsequent offshore direction, i.e. the phase lag effects (Dohmen-Jassen et al [6]). Based on above consideration, a

correction parameter k_{tr} is introduced to take such effect into account. Instead of applying the k_{tr} to both parts, however, the correction should be limited to the wave-induced transport only as it is directly affected by the phase-lag. As a result, the total transport rate can be summed up as follows:

$$q_s = \int_0^h \overline{u}_c \overline{C} dz + k_{tr}\left(\int_0^h \overline{u}_w \overline{C} dz\right) \quad (10)$$

Essentially, the wave-induced transport rate is reduced through a smaller k_{tr} value for fine sediment and short period waves. For coarser sediment and long period wave cases, the transport rate is less affected as k_{tr} being close to unity. Dohmen-Janssen *et al* [6]) suggest an analytical solution for k_{tr} based on a phase lag parameter p. The present study focuses on a combined sinusoidal oscillatory signal with a steady current, the formulation in Dohmen-Janssen *et al* [6] for the k_{tr} calculation can be written as:

$$k_{tr} = \frac{(U_c/U_\infty)^2 + 0.5 + F_1(P)}{(U_c/U_\infty)^2 + 1.5} \quad (11)$$

in which U_c is the steady current velocity, U_∞ is the wave orbital velocity magnitude, $F_1(P) = \frac{P_1 \cos\varphi_1 + Q_1 \sin\varphi_1}{\sqrt{P_1^2 + Q_1^2}}$, $P_1 = 0.5 + \left[\frac{1}{16} + p^2\right]^{1/4} \cos(0.5\alpha_1)$, $Q_1 = \left[\frac{1}{16} + p^2\right]^{1/4} \sin(0.5\alpha_1)$, $\alpha_1 = \arctan(4p)$, $\varphi_1 = \arctan(-Q_1/P_1)$ and the phase lag parameter $p = \frac{\varepsilon_s \omega}{w_f^2}$. It can be seen that the phase lag parameter p essentially describes the ratio between the sediment particle's falling time and the wave period. For fine sand under high speed flows and short period waves, the phase lag parameter p will be large. As a result of the large p, k_{tr} will be smaller than unity and therefore the total transport rate is reduced.

3.5. Graded Sediment

Apart from the sheet flow processes discussed above, the sediment size grading effects also have been recognised as an important factor associated with the transport prediction in the coastal area; see Li and Davies [17]. To deal with this problem, a multi-fraction approach is adopted in the present study in which bed material is divided into a number of fractions and each fraction is given a certain percentage occurrence based on the sand grading characteristics. The transport model is applied to each fraction and the total transport rate can then be calculated as the sum of the transport rate from all fractions.

In the first layer above the bed, it is assumed that the sediment is well mixed and the fraction of the undisturbed bed material is used within this layer. Such an assumption is purely for reason of simplicity and no theoretical consideration is given at this stage. A detailed description of partitions for each fraction would require a more complicated bed material sorting theory, which is still not available yet. Meanwhile, such an approach also avoids the involvement of any hiding and exposure functions, which is more questionable in sheet flow. The first layer thickness, however, is computed according to the mean grain size of the mixture rather than each fraction. Higher in the suspension layer, the sediment concentration is evaluated according to the procedures discussed previously for each fraction and the fraction occurrence is decided using a similar approach to that of Zyserman et al [39]. In this way, the integrated suspended transport of each fraction is equal and the percentage of occurrence for the fine sand therefore would be smaller than that for the coarse sand due to its higher concentration values.

Although both WPA velocities and sediment concentration in Eq.(3), Eq.(5) and Eq.(9) are all based on analytical expressions, the vertical integration that needed in the computation of total transport rate still requires numerical discretisation across the water depth. However, such integration is straightforward in its implementation and computationally efficient in comparison with other methods using complex numerical solution approach. Sensitivity tests have shown that minimum 7 layers would be required if a uniform grid size is used. With spatially varying grids, the total number of layers can be further reduced.

Table 1. Test conditions and eddy viscosity reduction parameter of β_c for the LOWT cases.

Case	D_{50} (mm)	U_∞ (m/s)	U_c (m/s)	β_c (-)
E2	0.210	1.35	0.20	0.30
H6	0.130	1.47	0.23	0.20
H9	0.130	0.90	0.44	0.40
H44	0.130	1.10	0.23	0.50
H412	0.130	1.10	0.23	0.30
I1	0.320	1.50	0.23	0.90
K5	0.194	1.50	0.25	0.30
O7	0.130	1.10	0.33	0.45
O8	0.130	1.10	0.40	0.40

4. Model calibration

In previous sections, a number of coefficients were introduced in the model to represent various transport mechanisms, which have to be validated against available measurements before they can be used for general application. In total, nine laboratory tests conducted at the LOWT in Delft Hydraulics for combined wave-current sheet flows were used for such validations, namely tests E2, H6, H9, H44, H412, I1, K5, O7 and O8. Sediment sizes in these experiments were fine (0.13mm), medium (0.21mm) and coarse sand (0.32mm), and the relative strength of the current to the wave orbital motion also ranged from 0.15 up to 0.5. Detailed experimental conditions for these tests and the related sediment characteristics are given in the above Table 1.

4.1. Eddy viscosity parameter β_c

To find a proper value for the eddy viscosity parameter β_c in Eq. (2), the model was applied to the calibration cases listed in Table 1. During these tests, β_c was tuned for each case until the best agreement between the computed and measured flow velocity profiles is obtained. Typical results for such comparisons are shown in Fig 4. It was found that except H412 and O7, the model predictions follow the measurements very well. The enhanced bed roughness and the velocity variation across the boundary layer under combined waves and current have been properly represented. The divergences at low elevations in H412 and O7 may suggest that the model over-predicts the boundary layer thickness for the fine sand in these two cases. This is partly due to the over predicted roughness height from Eq. 4 for these two cases. The obtained β_c value for each case is also listed in Table 1. Except for the very coarse material in I1, it was found that the variation of β_c value in these cases is small, around 0.2 – 0.5 for both medium and fine sand. The high value in I1 appears to suggest less turbulence damping effects for the coarse material. An averaged value for the above cases, 0.35, is used in the present model, which is in the similar range to the findings (0.08-0.5) in Dohmen-Janssen *et al* [6].

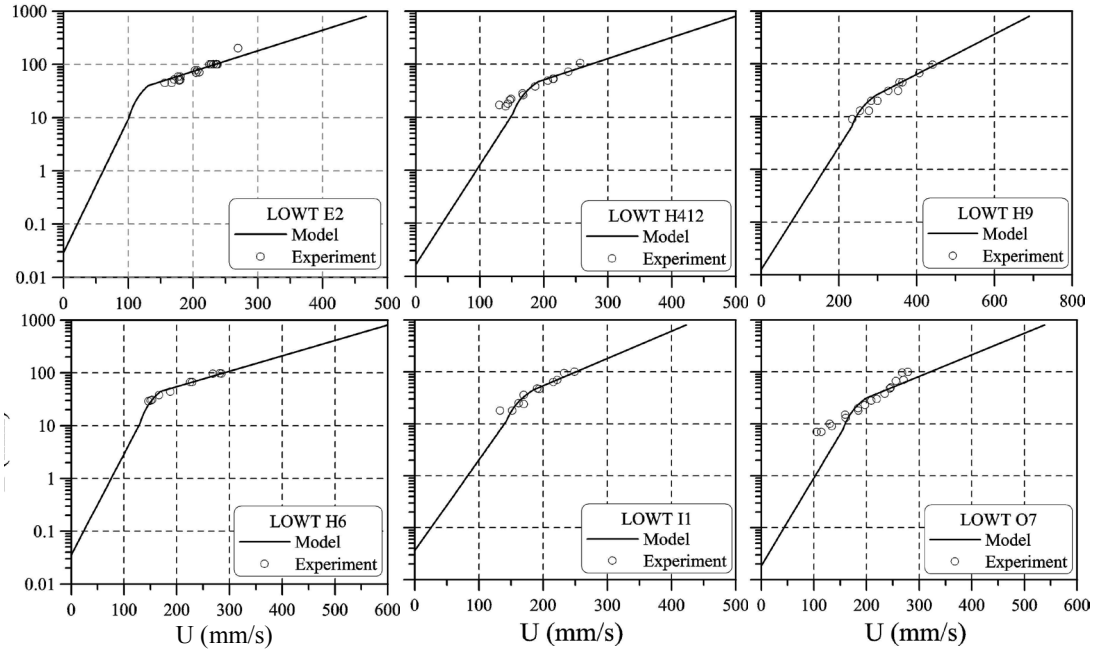

Figure 4. Comparison of computed WPA current velocity with LOWT measurements.

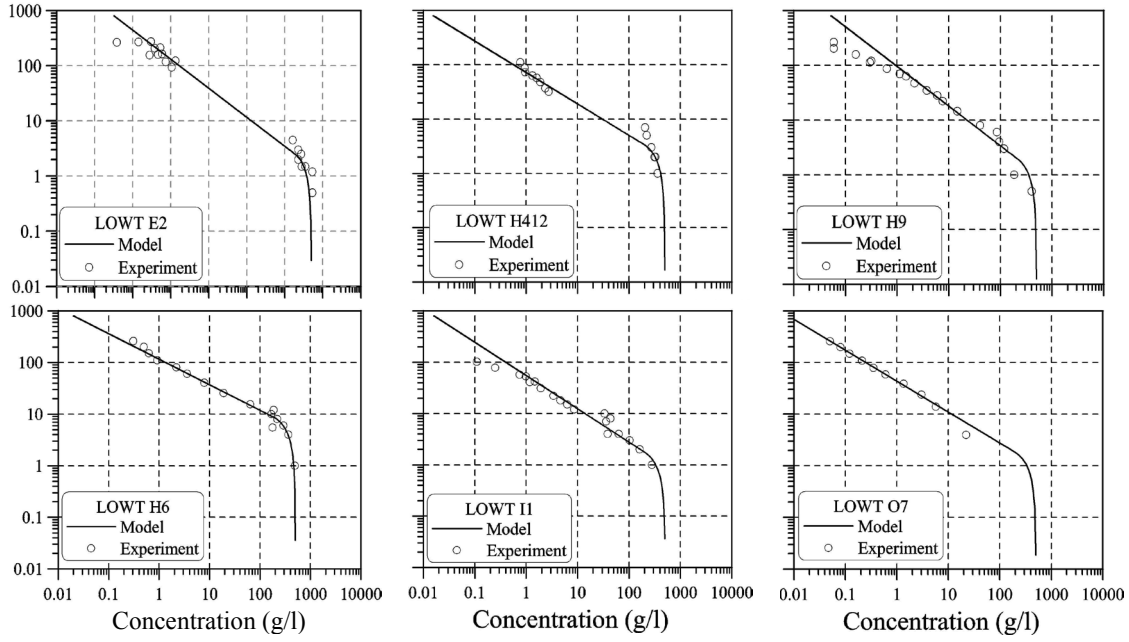

Figure 5. Comparison of computed WPA sediment concentration with LOWT experimental data

4.2. Sediment Diffusivity Parameter β_S and Sheet Flow Layer Thickness D_s

To determine values for β_s and the first layer thickness d_s, the model was run for the nine calibration cases in which these two parameters were tuned for each case so that the predicted concentration profile is able to match with the measurements, similar to the calibration procedure for β_c. Typical results are shown in Fig 5. It is found that computed profiles are able to follow with the measurements very well, especially for the medium and coarse sand even at very low level in the sheet flow layer.

The β_s values obtained from these calibration cases are presented in Fig 6, together with the values predicted by van Rijn [34] and Rose and Thorne [22]. The figure shows that for small u_{sw}/w_f, the present method predicts much lower value of β_s than these two previous studies. This is primarily due to that fact that the present model concentrates on sheet flow regime while these two previous studies were designed for study of tidal flow. It should be pointed out that w_f in the present study refers to the fall velocity in quiescent water, not in the sediment-laden turbulent flow. An approximation to the present model results can be found as following formula, which is shown in Fig 6 by the solid line:

$$\beta_s = 1 + \frac{1}{2}\left[\frac{w_f}{u_{sw}}\right]^2 \tag{12}$$

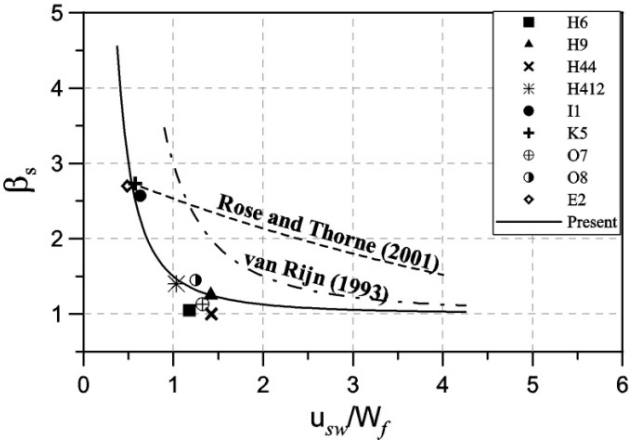

Figure 6. Sediment diffusivity reduction parameter βs values for LOWT tests.

In Fig 7, the d_s values normalised by medium grain size are presented against the shear parameter θ. A fit of the data is found for fine and medium sand as follows:

$$\frac{d_s}{D_{50}} = 5.8e^{0.41\theta} \tag{13}$$

Value of d_s computed from Eq. (10) are substantially lower than these suggested by Dohmen-Janssen *et al* [6] for a sheet flow layer thickness. This is due to the fact that the d_s defined in the present study is that part of the sheet flow layer above the undisturbed initial bed level (z > 0), while δ_s in Dohmen-Janssen *et al* [6] includes the portion below z = 0 level.

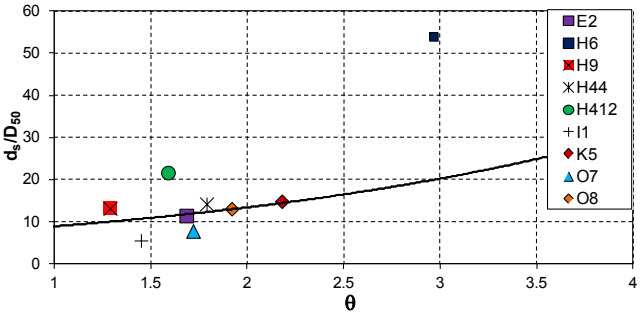

Figure 7. Normalised first layer thickness d_s used in LOWT tests.

4.3. Wave-Induced Residual Velocity Parameter α

To verify the wave residual velocity parameter α in Eq. (6), the computed wave related transport flux are compared with the measurements of E2, I1, H6 and H9 in Fig 8(b). The corresponding current-induced transport flux is shown in Fig 8(a). As expected, the current-related transport rates in the medium (E2) and coarse (I1) sand cases follow the measurements very well. The agreements for two fine sand cases (H6 and H9) close to the bed are also reasonable. The accuracy of the wave related transport rates generally are regarded to be satisfactory for these two medium and coarse sandy cases. In the fine sand cases (H6 and H9), a large onshore transport is found close to the zero level. Unfortunately, no detailed measurements are available within this region to verify the predictions. However, the good agreement in the total transport rate in the later section seems confirm these values.

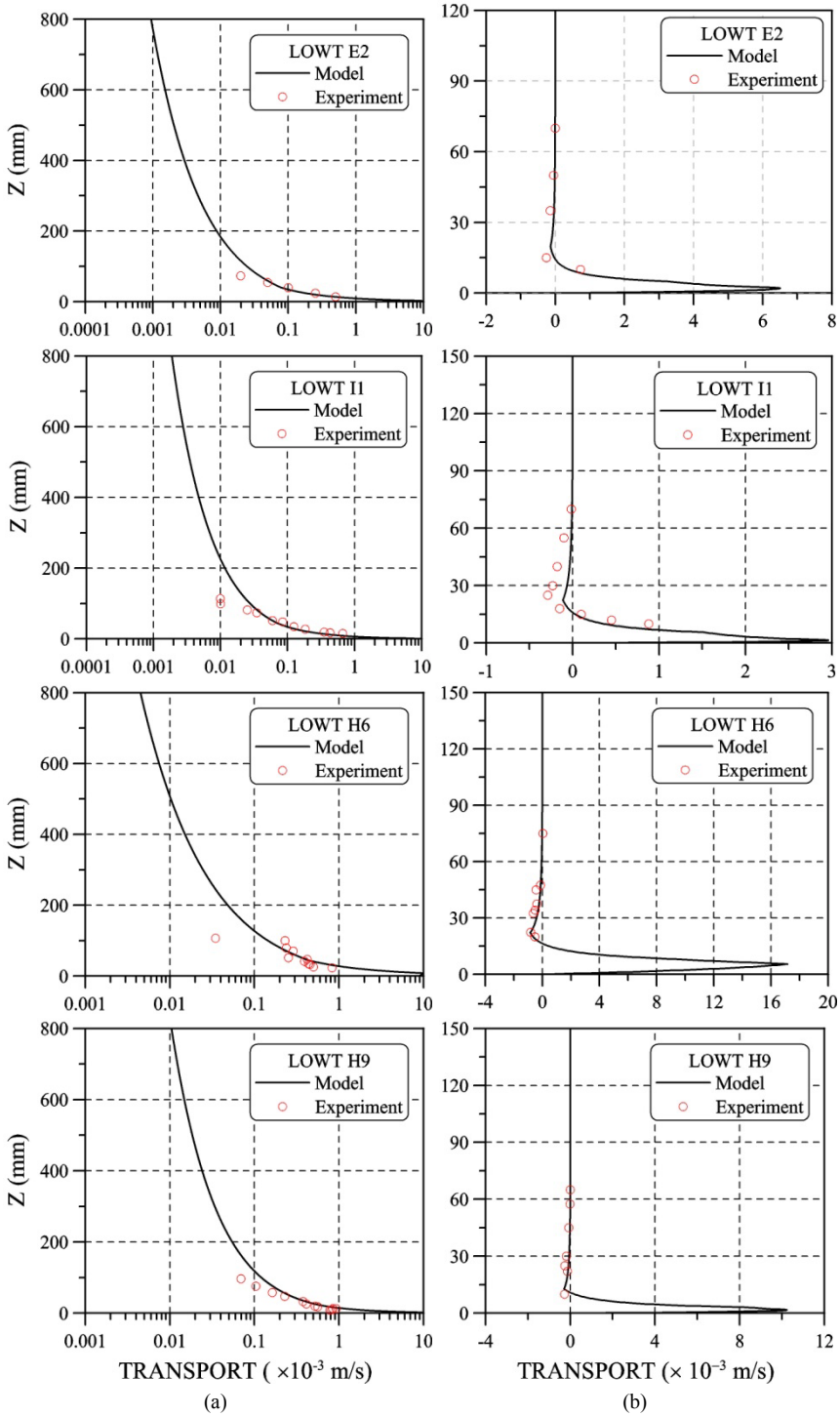

Figure 8. Comparison of the computed current related (a) and wave related (b) transport rates against LOWT measurements.

5. Model Application and Results

After the parameters of β_c, β_s, k_{tr}, α and d_s being verified based on the nine calibration cases, the model was further tested against other available laboratory measurements from LOWT, including series E, H, I, J and K. Measurements of sediment suspension under propagating waves on a natural beach in the EU MAST project COAST3D (van Goor et al [32]) were also used to test the model's predictions under field condition. Details of these LOWT test conditions can be found in various publications, e.g. Katopodi et al [14], Ribberink and Al-Salem [21], Janssen et al [12], Hamm et al [10], Dohmen-Janssen et al [6] and Trouw et al [27]). Table 2 lists the conditions of the six field cases from the COAST3D database for the model testing.

Table 2. Experimental conditions for field measurements of van Goor *et al*.

Experiment	h (m)	H_s (m)	T (s)	U_c (m/s)
5B	0.98	0.45	3.71	-0.07
6A	0.90	0.48	4.05	-0.10
12B	0.81	0.34	5.47	0.39
14B	1.04	0.33	3.31	0.32
15A	0.67	0.47	12.01	-0.47
16A	0.67	0.41	9.12	-0.45

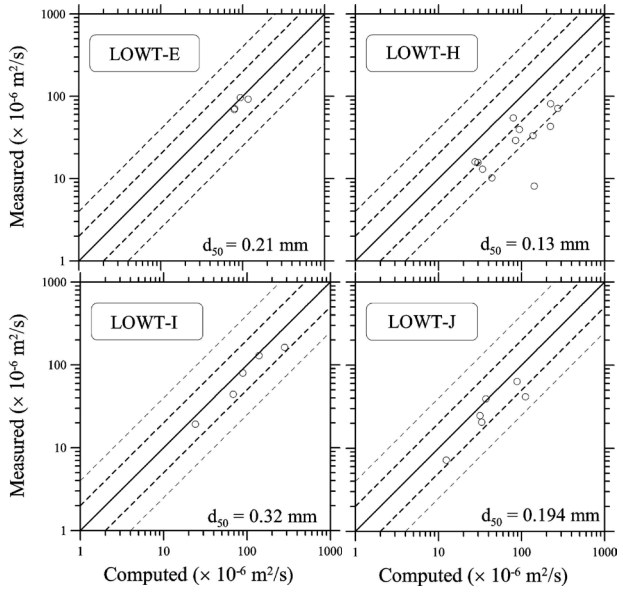

Figure 9. Comparison of computed total transport rates against measurements for LOWT cases.

5.1. LOWT laboratory tests (uniform sand)

Fig 9 presents the comparison between the computed total transport rates and the measured values for the LOWT series (E H, I and J) involving uniform sand. In all of these calculations, the k_{tr} parameter was kept at unity firstly. Overall, it is found that for medium and coarse sand, the predictions are generally within ±100% of the measured values. For fine sand, i.e. H series, most of the predicted values fall within ±100% ~ ±200% of the measurements Such divergence partly comes from the over-prediction of wave-related transport in the onshore direction for the fine sediment, which is primarily associated with the lack of phase lag effect as discussed previously.

Using the k_{tr} computed from Eq. (13), the total transport rates for the H series were recalculated and compared with the measurements in Fig 10(b). The original result from Fig 9 is also shown in Fig 10(a) as a comparison. It is evident that the accuracy of the predicted total transport rates for fine sand in these cases is comparable with that for medium and coarse sand as shown in Fig 9, in which more than 75% of the results are well within ±100%. Given the very simple approach used in the present study for the prediction of fine sediment transport under complex sheet flow, such accuracy is regarded as acceptable. A better agreement for the fine sediment materials will require a more detailed description of the phase lag effects on the transport parameter k_{tr} as well as the residual velocity profile parameter α. It is yet possible to carry out such calibration based on the existing limited amount of high quality measuring data for the combined waves with current-induced sheet flow. Results from more sophisticated models, such as the two phase numerical model of Li *et al* [16], will be able to provide more insight into a possible parameterisation of these coefficients as future studies.

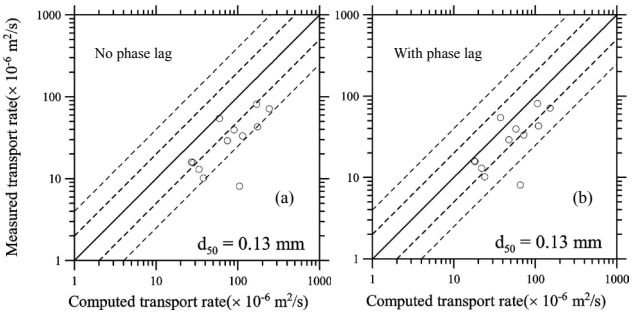

Figure 10. Comparison of predicted total transport rates with LOWT measurements (H series): in (a) Model are based on k_{tr} = 1; in (b) based on k_{tr} is computed based on Eq. (15).

5.2. LOWT Laboratory Tests (Graded Sand)

One set of graded sediment experiments in the LOWT database, series K, was also simulated to test the multi-fraction method in the present model. The sediment material was simply divided into two fractions according to the experiment, a fine sand fraction with d_{50} = 0.13mm and a coarse sand fraction with d_{50} = 0.32mm. The bed material is comprised of 50% of each fraction.

Fig 11 shows the computed and measured concentration profile across the depth. The β_s values obtained from the calibration in Eq. (2) were used for both the fine and coarse fractions. It is clear that the concentration in the lower level of the sheet flow layer is dominated by a high concentration of the mixture with the curve slope near horizontal, whereas at the higher level above 4mm the concentration curve shows an apparently larger slope which is believed to be dominated by fine sand with a smaller settling velocity than the coarse sand. Such a distribution can also be verified by the percentage occurrence for the material in suspension based on the concentration of each fraction as shown in Table 3, together with the measured values as a comparison. In general, the agreements are considered to be good which also justify the above expression for β_s value for fine sand in Fig 6. Similar good agreement was also found for test K6 as presented in Table 3.

The computed total transport rates for K5 and K6 based on both single-fraction and multi-fraction approaches are also compared with the measurements in Fig 12 It is evident that the multi-fraction method has improved the prediction on average up to 35%. However, due to the largely over-predicted transport rate for the fine sand in general, the model's results are still higher than those of the laboratory

data for these two cases.

Table 3. Computed and measured percentage of fine and coarse sand size in suspension for K5 and K6.

Case	Fine sand (%)		Coarse sand (%)	
	Measured	Computed	Measured	Computed
K5	65.82	67.31	34.18	32.69
K6	65.33	71.76	34.67	28.24

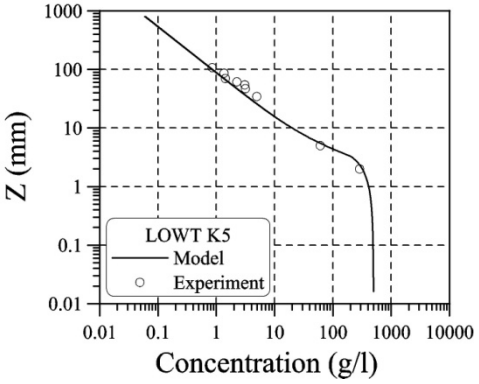

Figure 11. Comparison of computed sediment concentration using multi-fraction approach with measurements for LOWT K5 case.

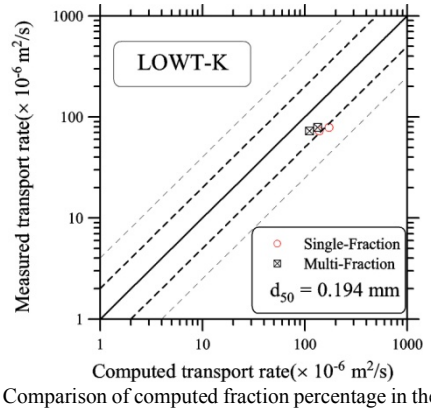

Figure 12. Comparison of computed fraction percentage in the suspension layer for K5 and K6 test with the measured values.

5.3. Field Tests (Egmond)

In the COAST3D project (van Goor *et al* [32]), detailed measurements of sediment suspension under propagating waves on a straight beach at Egmond aan Zee, the Netherlands have been carried out. In total, six cases from these experiments were used for the present model's test at field scale. During the experiments, the sand on the beach had a medium size with d_{50} = 0.3mm and d_{90}=0.5mm (Table 2).

In these cases, the random seas are represented by significant wave height H_s and peak period T_p, which are used directly in the calculation as the representative wave height and period for the estimation of near bed free-stream velocity and other quantities based on linear wave theory.

The computed sediment transport rates for these six cases are compared with the measurements in Fig 13, together with the results from the commonly used methods of Bijker [1] and Soulsby [26]. All predictions based on present method are within ±100% of the measurements as indicated in the figure, which demonstrated the model's ability for prediction of sediment transport in field conditions. In comparison, the Bijker approach appears has the largest deviation from the measurements and tend to under estimate the transport rate for those lower values. The Soulsby method performs better than Bijker but tends to underestimate most of the transport rates. However, it should also bear in mind that many other processes, such as wave breaking, boundary layer streaming and longshore currents have not yet been included in the present model. As a result, only a limited number of experimental cases can be used for the present model's test. It is therefore necessary to further improve the model so that it can be applied to more general field conditions directly.

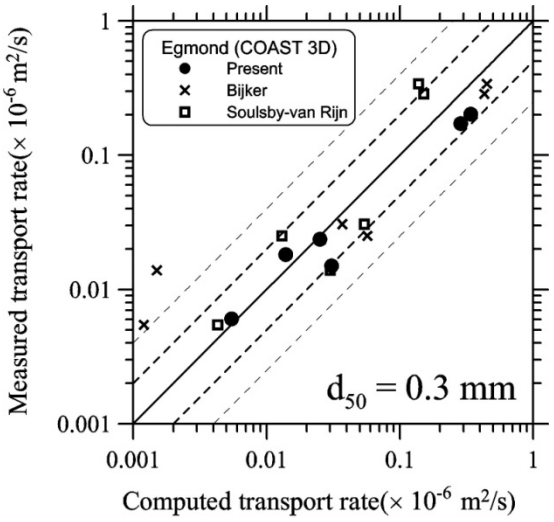

Figure 13. Comparison of predicted and measured sediment total transport rates for COAST3D field data (van Goor *et al* 2001).

6. Discussions

The present study aims to establish a sediment transport prediction model for combined wave-current flows based on WPA quantities, taking into account sufficient oscillatory sheet flow layer processes. Following a number of previous studies, the WPA velocity profile is computed based on two connected logarithmic profiles and the corresponding sediment concentration is determined by a two-layer approach. Turbulence damping and sediment-fluid interactions are represented simply by a fluid eddy viscosity factor β_c and a sediment diffusivity factor β_s, which have been validated through the use of LOWT experimental results.

A wave residual flow velocity profile was also proposed so that an approximation to the wave-related transport rate can be computed based on such a profile and the wave-period-averaged sediment concentrations. Comparisons between model results and the available measurements for the total sediment transport rate are considered to be satisfactory for coarse and medium sand. The inclusion of a phase lag parameter p also considerably improved the model's predictions for the total sediment

transport rate for fine sand. It is therefore recognised that phase lag effects have to be taken into account in practical predictions, particularly for fine sediment. The multi-fraction method adopted in the present study yields good agreement with the measured fraction partition in a graded sediment test. Compared with a single fraction approach, the prediction of total transport rate based on such a method also has been improved. Model tests against measurements from a field campaign also show good accuracy.

7. Conclusions

Based on the results from the present study, several conclusions can be drawn as follows:

1) The WPA approach for wave-current induced flow velocity and eddy viscosity profiles are applicable to sheet flows given the important processes, including wave asymmetry, sheet flow layer process and particle-flow interactions are included in the formulation.
2) The diffusion-type of net sediment concentration profile also is applicable to the wave-current sheet flows with particular considerations of sheet flow layer.
3) The net transport rate can be reasonably predicted based on the above WPA velocity profile and sediment concentration profile. However, the important wave-induced transport should also be included.
4) For the practical applications, the size grading effect is particularly important for mixture sediments.
5) Due to the composition of the present model, cases involve current only condition can also be dealt with by ignoring the wave influences on the flow velocity profile and sediment concentration. For wave only cases, the wave-induced WPA velocity profile in Eq.5 can still be applied and hence for asymmetrical waves, the difference in onshore and offshore transport fluxes will then decide the net transport rate.
6) However, as all parameters involved in the present study are calibrated against measurements in sheet flow regime, the applicable range of the model therefore is for cases in which mobility number is larger than 1.0. For the lower flow regime, the present model concept is still applicable, but the parameters involved should be further validated.
7) It is also recognised that limited number of model verifications have been carried out and further calibrations and parameterisations are still needed in order to enable the present model to be used for general engineering design work.

Acknowledgements

This research was financially supported by Engineering and Physical Sciences Research Council U.K., under contract number Grants GR/R23596(LUBA) and EP/J005541/1(SINBAD).

REFERENCES

[1] Bijker, W. (1967) Some considerations about scales for coastal models with movable bed, Delft Hydraulics Lab. Publication, 50 pages.

[2] Davies, A. and Villaret, C. (1999) Eulerain drift induced by progressive waves above rippled and very rough beds, Journal of Geophysical Research, 104(C1),1465-1488.

[3] de Meijer, R. J., Bosboom, J., Cloin, B., Katopodi, I., Kitou, N., Kommans, R. L. and Manso, F., (2002) Gradation effects in sediment transport, Coastal Engineering, 47, 179-210.

[4] Dibajnia, M. and Watanabe, A, (1991) Sheet flow under nonlinear waves and currents, Proceedings 23rd International Conference on Coastal Engineering, ASCE, Venice, 2015-2028.

[5] Dohmen-Janssen, M., (1999) Grain size influence on sediment transport in oscillatory sheet flow, Technische Universiteit Delft, Ph.D.

[6] Dohmen-Janssen, M., Kroekenstoel, D. F., Hassan, W. N. and Ribberink, J. S., (2002) Phase lags in oscillatory sheet flow: Experiments and bed load modelling, Coastal Engineering, 46, 61-87.

[7] Dong, P. and Zhang, K., (1999) Two-phase flow modelling of sediment motions in oscillatory sheet flow, Coastal Engineering, 36, 87-109.

[8] Fredsøe, J., (1984) Turbulent boundary layer in wave-current motion, Journal of Hydraulic Engineering, ASCE, 110(HY8), 1103-1120.

[9] Grasmeijer, B. T., Chung, D. H. and van Rijn, L. C., (1999) Depth-integrated sand transport in the surf zone, Coastal Sediments '99, ASCE, Hauppauge, Long Island, New York, 325-340.

[10] Hamm, L., Katopodi, I., Dohmen-Janssen, M., Ribberink, J., Samothrakis, P., Cloin, B., Savioli, J., Chatelus, Y., Bosboom, J., Nicholson, J. and Hein, R. (1998) Grain size and gradation effects on sediment transport processes in oscillatory flow conditions, Delta Hydraulics, Data Report Z2153.

[11] Hsu, T., Chang, H. and Hsieh, C. (2003) A two-phase flow model of wave-induced sheet flow, Journal of Hydraulic Research, 41(3), 299-310.

[12] Janssen, C. M., Hassan, W.N., van der Wal, R. J. and Ribbrtink, J. S. (1996) Net sand transport rates and transport mechanisms of fine sand in combined wave-current sheet flow conditions, Delft Hydraulics, Data Report H2462, Part IV.

[13] Kaczmarek, L. M., (1999) Moveable sea bed boundary layer and mechanics of sediment transport, Institute of Hydroengineering of the Polish Academy of Sciences, Ph.D.

[14] Katopodi, I., Ribberink, J.S., Roul, P., Koelewijn, R., Lodahl,

C., Longo, S., Crosato, A., and Wallace, H., (1994) Intra-wave sediment transport in an oscillatory flow superimposed on a mean current, Data Report H1684, Part III, WL|Delft Hydraulics, NL.

[15] Li, L. and Sawamoto, M. (1995) Multi-phase model on sediment transport in sheet flow regime under oscillatory flow, Coastal Engineering in Japan, 38, 157-178.

[16] Li, M., Pan, S. and O'Connor, B. A., (2008) A two phase numerical model for sediment transport prediction under oscillatory sheet flows, Coastal Engineering, 55(12), 1159-1173.

[17] Li, Z. and Davies, A., (1996) Towards predicting sediment transport in combined wave-current flow, Journal of Waterway, Port, Coastal and Ocean Engineering, ASCE, 122(4), 157-163.

[18] Malarkey, J., Davies, A. and Li, Z., (2003) A simple model of unsteady sheet-flow sediment transport, Coastal Engineering, 48, 171-188.

[19] O'Connor, B. A. and Yoo, D., (1988) Mean bed friction of combined wave-current flows, Coastal Engineering, 12, 1-21.

[20] O'Donoghue, T. and Wright, S., (2003) Concentrations in oscillatory sheetflow for well sorted and graded sands, Coastal Engineering, 50, 117-138.

[21] Ribberink, J.S. and Al-Salem, A.A., (1995) Sheet flow and suspension of sand in oscillatory boundary layers, Coastal Engineering, 25, 205-225.

[22] Rose, C. P. and Thorne, P., (2001) Measurements of suspended sediment transport parameters in a tidal estuary, Continental Shelf Research, 21, 1551-1575.

[23] Ruessink, B.G., van den Berg, T. and van Rijn, L. (2009) Modeling sediment transport beneath skewed asymmetric waves above a plane bed, Journal of Geophysical Research, 114(C11021), doi:10,1029/2009JC005416.

[24] Savioli, J. and Justesen, P. (1997) Sediment in oscillatory flows over plane bed, Journal of Hydraulic Research, 35(2), 177-190.

[25] Sleath, J., (1991) Velocities and shear stresses in wave-current flows, Journal of Geophysical Research, 96(C8), 15237-15244.

[26] Soulsby, R., (1997) Dynamics of marine sands: A manual for practical applications, HR Wallingford, U.K. Report No.SR 466.

[27] Trouw, K., Cloin, B., Arnott, A., Hassan, W., Dong, P., van de Graaff, J., Rose, C., Ribberink, J. and Sistermans, P. (2001) Vertical sediment entrainment characteristics in oscillatory sheet flow conditions, Delft Hydraulics, Data Report Z2454.

[28] van der A, D., O'Donoghue, T. and Ribberink, J. (2009) Sheet flow transport process in oscillatory flow with acceleration skewness, Proceedings Of Coastal Dynamics 2009, Impacts of Human Activities on Dynamic Coastal Processes, World Scientific Publishing, doi: 10.1142/9789814282475_0132.

[29] van der A, D., O'Donoghue, T. and Ribberink, J. (2010) Measurements of sheet flow transport in acceleration-skewed oscillatory flow and comparison with practical formulations, Coastal Engineering, 57, 331-342.

[30] van der A, D., Ribberink, J., van der Werf, J. and O'Donoghue, T. (2010) New practical model for sand transport induced by non-breaking waves and currents. Proceedings of 30th International Conference on Coastal Engineering, Shanghai, China, World Scientific Publishing.

[31] van der Werf, J., Nomden, H., Ribberink, J., Walstra, D. and Kranenburg, W. (2012) Application of a new sand transport formula with the cross-shore morphodynamic model UNIBEST-TC, Proceedings of 31st International Conference on Coastal Engineering, World Scientific Publishing.

[32] van Goor, M. A., Sistermans, P. G. and van Rijn, L. C., (2001) SEDMOC database TAP and TAPS, SEDMOC: Sediment transport modelling in marine coastal environments, van Rijn, L. C., Davies, A., van de Graaff, J. and Ribberink, J. S., Amsterdam, AQUA Publications, AA1-AA5.

[33] van Rijn, L. C., (1989) Handbook of sediment transport by currents and waves, Delft Hydraulics, The Netherlands, Report No.H461

[34] van Rijn, L. C., (1993) Principles of sediment transport in rivers, estuaries and coastal seas, Aqua Publications.

[35] van Rijn, L. C., Soulsby, R., Hoekstra, H. and Davies, A. (2005) SANDPIT: Sand transport and morphology of offshore mining pits, Aqua Publications, Amsterdam, The Netherlands.

[36] You, Z., (1994) A simple model for current velocity profiles in combined wave-current flows, Coastal Engineering, 23, 289-304.

[37] You, Z., Wilkinson, D. and Nielson, P., (1991) Velocity distributions of waves and currents in the combined flow, Coastal Engineering, 15, 525-543.

[38] Yu, X., Hsu, T., Jenkins, J. and Liu, P. (2012) Predictions of vertical sediment flux in oscillatory flows using a two-phase, sheet flow model, Advances in Water Resources, 48, 2-17.

[39] Zyserman, J. A., Savioli, J. C. and Jensen, J. H., (2002) Modeling transport of sediment mixtures in current and waves, 28th International Conference on Coastal Engineering. ASCE, Cardiff, 2465-2477.